ECE 796:

Models of the Neuron

Slides for Lecture #1

Friday, January 12, 2007

Model

OED definition:

> “A simplified or idealized description or conception of a particular system, situation, or process (often in mathematical terms: so mathematical model) that is put forward as a basis for calculations, predictions, or further investigation.”

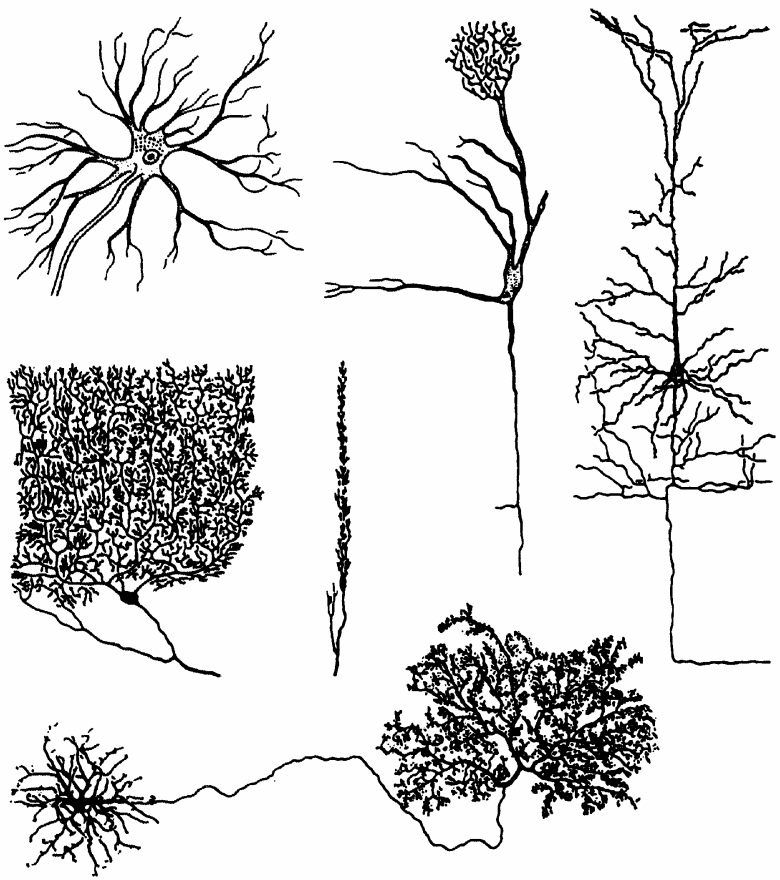

Figure 1.1 Examples of neurons in the nervous system exhibiting various morphology. From the upper left in clockwise order: motor neuron from the spinal cord, mitral cell from olfactory bulb, pyramidal cell from cortex, horizontal cell from retina, and Purkinje cell (front and side views) from cerebellum. (From Nicholls et al. 1992 and Fisher and Boycott 1974.)

(from Johnston and Wu)

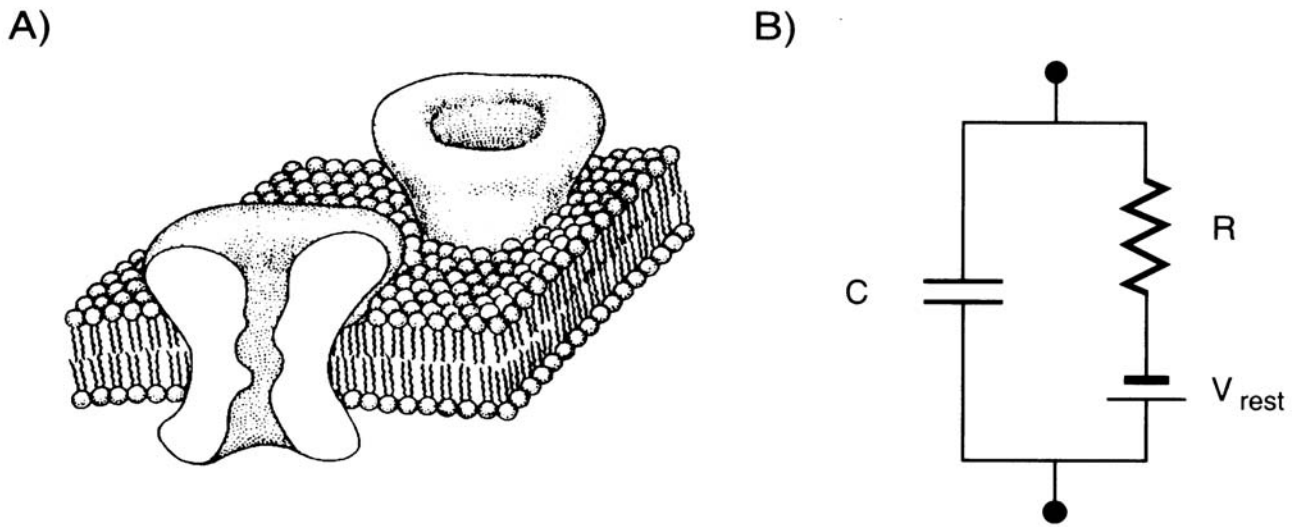

Fig. 1.1 NATURE OF THE PASSIVE NEURONAL MEMBRANE **(A)** Schematic representation of a small patch of membrane of the types enclosing all cells. The 30–50 Å thin bilayer of lipids isolates the extracellular side from the intracellular one. From an electrical point of view, the resultant separation of charge across the membrane acts akin to a capacitance. Proteins inserted into the membrane, here ionic channels, provide a conduit through the membrane. Reprinted by permission from Hille (1992). **(B)** Associated lumped electrical circuit for this patch, consisting of a capacitance and a resistance in series with a battery. The resistance mimics the behavior of voltage-independent ionic channels inserted throughout the membrane and the battery accounts for the cell's resting potential V_{rest}.

(from Koch)

Table 2.1 Ion concentrations and equilibrium potentials

	Inside (mM)	Outside (mM)	Equilibrium Potential (NE) $E_i = \frac{RT}{zF} \ln \frac{[C]_{out}}{[C]_{in}}$
Frog muscle (Conway 1957)			$T = 20°C = 293°K$
K^+	124	2.25	$58 \log \frac{2.25}{124} = -101$ mV
Na^+	10.4	109	$58 \log \frac{109}{10.4} = +59$ mV
Cl^-	1.5	77.5	$-58 \log \frac{77.5}{1.5} = -99$ mV
Ca^{2+}	$4.9^\dagger$	2.1	$29 \log \frac{2.1}{10^{-4}} = +125$ mV
Squid axon (Hodgkin 1964)			
K^+	400	20	$58 \log \frac{20}{400} = -75$ mV
Na^+	50	440	$58 \log \frac{440}{50} = +55$ mV
Cl^-	40–150	560	$-58 \log \frac{560}{40-150} = -66 - (-33)$ mV
Ca^{2+}	$0.4^\dagger$	10	$29 \log \frac{10}{10^{-4}} = +145$ mV
Typical mammalian cell			$T = 37°C = 310°K$
K^+	140	5	$62 \log \frac{5}{140} = -89.7$ mV
Na^+	5–15	145	$62 \log \frac{145}{5-15} = +90.7 - (+61.1)$ mV
Cl^-	4	110	$-62 \log \frac{110}{4} = -89$ mV
Ca^{2+}	$1–2^\dagger$	2.5–5	$31 \log \frac{2.5-5}{10^{-4}} = +136 - (+145)$ mV

$^\dagger(10^{-4})$ free

(from Johnston and Wu)

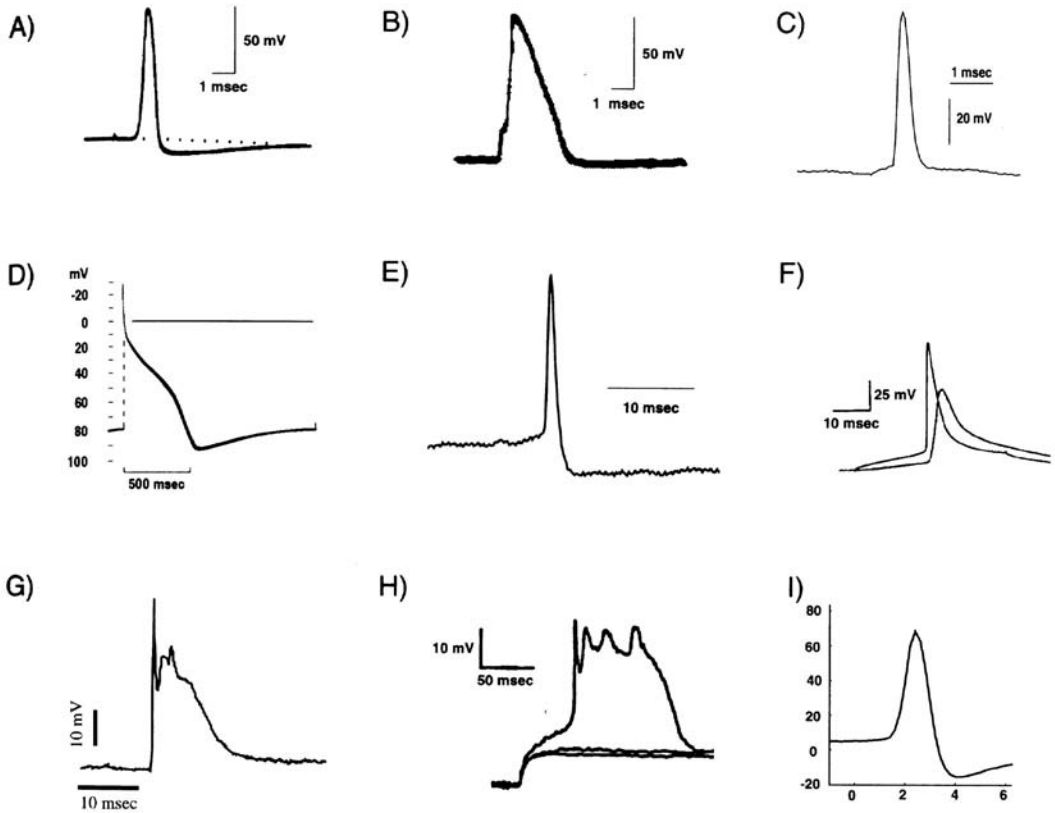

Fig. 6.1 ACTION POTENTIALS OF THE WORLD Action potentials in different invertebrate and vertebrate preparations. Common to all is a threshold below which no impulse is initiated, and a stereotypical shape that depends only on intrinsic membrane properties and not on the type or the duration of the input. **(A)** Giant squid axon at 16° C. Reprinted by permission from Baker, Hodgkin, and Shaw (1962). **(B)** Axonal spike from the node of Ranvier in a myelinated frog fiber at 22° C. Reprinted by permission from Dodge (1963). **(C)** Cat visual cortex at 37° C. Unpublished data from J. Allison, printed with permission. **(D)** Sheep heart Purkinje fiber at 10° C. Reprinted by permission from Weidmann (1956). **(E)** Patch-clamp recording from a rabbit retinal ganglion cell at 37° C. Unpublished data from F. Amthor, printed with permission. **(F)** Layer 5 pyramidal cell in the rat at room temperatures. Simultaneous recordings from the soma and the apical trunk. Reprinted by permission from Stuart and Sakmann (1994). **(G)** A complex spike—consisting of a large EPSP superimposed onto a slow dendritic calcium spike and several fast somatic sodium spikes—from a Purkinje cell body in the rat cerebellum at 36° C. Unpublished data from D. Jaeger, printed with permission. **(H)** Layer 5 pyramidal cell in the rat at room temperature. Three dendritic voltage traces in response to three current steps of different amplitudes reveal the all-or-none character of this slow event. Notice the fast superimposed spikes. Reprinted by permission from Kim and Connors (1993). **(I)** Cell body of a projection neuron in the antennal lobe in the locust at 23° C. Unpublished data from G. Laurent, printed with permission.

(from Koch)

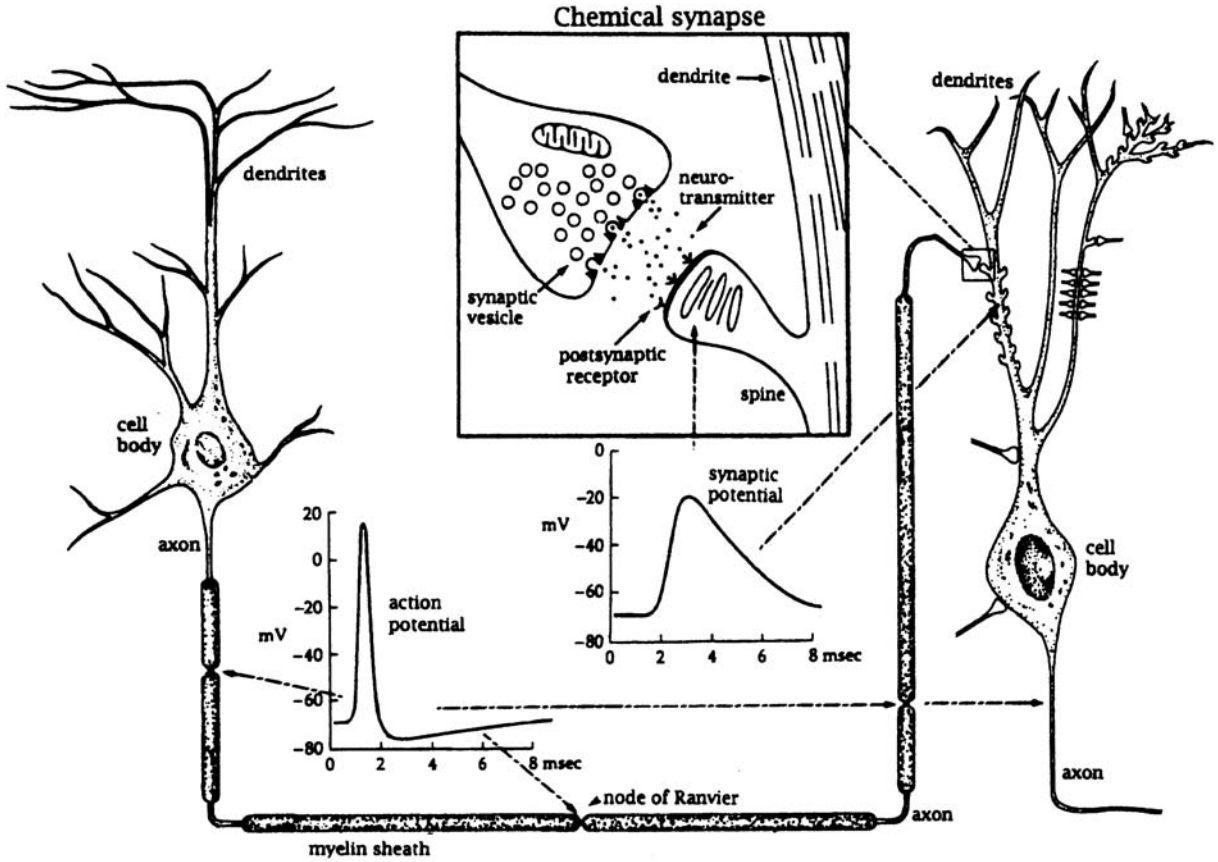

Figure 1.2 Neurons convey information by electrical and chemical signals. Electrical signals travel from the cell body of a neuron (left) to its axon terminal in the form of action potentials. Action potentials trigger the secretion of neurotransmitters from synaptic terminals (upper insert). Neurotransmitters bind to postsynaptic receptors and cause electric signals (synaptic potential) in the postsynaptic neuron (right). Synaptic potentials trigger action potentials, which propagate to the axon terminal and trigger secretion of neurotransmitters to the next neuron. (Adapted from Kandel et al. 1991 and from L.L. Iversen, copyright © 1979 by Scientific American, Inc. All rights reserved.)

(from Johnston and Wu)

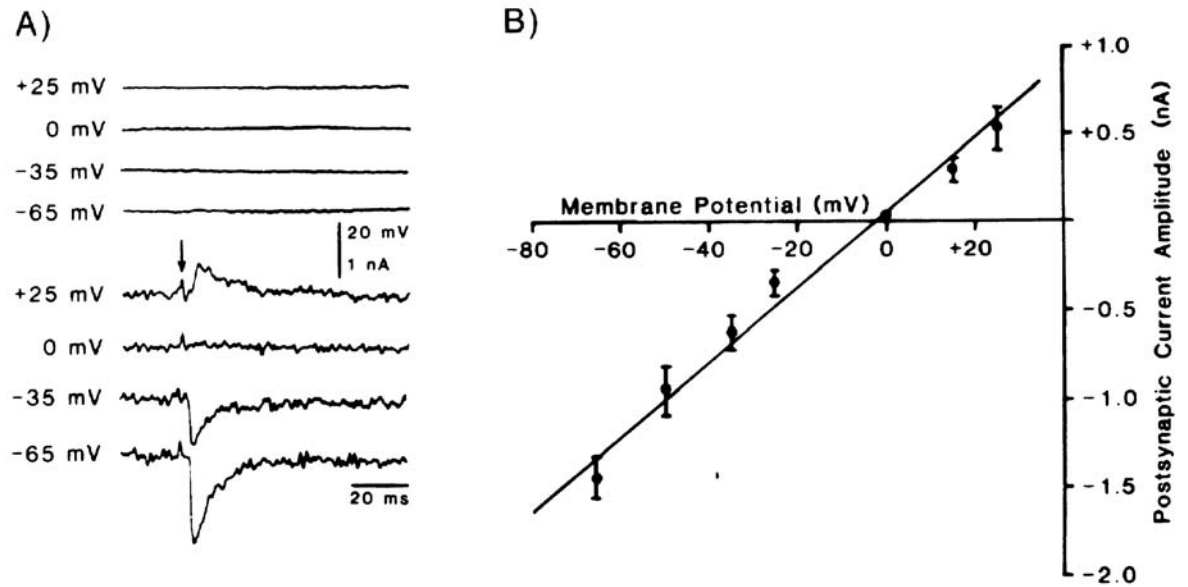

Fig. 1.6 A Fast Excitatory Synaptic Input Excitatory postsynaptic current (EPSC) caused by the simultaneous activation of synapses (arrow) made by the mossy fibers onto CA3 pyramidal cells in the rodent hippocampus (Brown and Johnston, 1983). This classical experiment showed how a central synapse can be successfully voltage clamped. **(A)** The voltage-clamp setup stabilizes—via electronic feedback control—the membrane potential at a fixed value. Here four experiments are shown, carried out at the holding potentials indicated at the left. The current that is drawn to keep the membrane potential constant, termed the clamp current, corresponds to the negative EPSC. It is maximal at negative potentials and reverses sign around zero. The synaptic current rises within 1 msec to its peak value, decaying to baseline over 20–30 msec. The experiments were carried out in the presence of pharmacological agents that blocked synaptic inhibition. **(B)** When the peak EPSC is plotted against the holding potential, an approximately linear relationship emerges; the regression line yields an x-axis intercept of -1.9 mV and a slope of 20.6 nS. Thus, once the synaptic reversal potential is accounted for, Ohm's law appears to be reasonably well obeyed. We conclude that synaptic input is caused by a transient increase in the conductance of the membrane to certain ions. Reprinted by permission from Brown and Johnston (1983).

(from Koch)

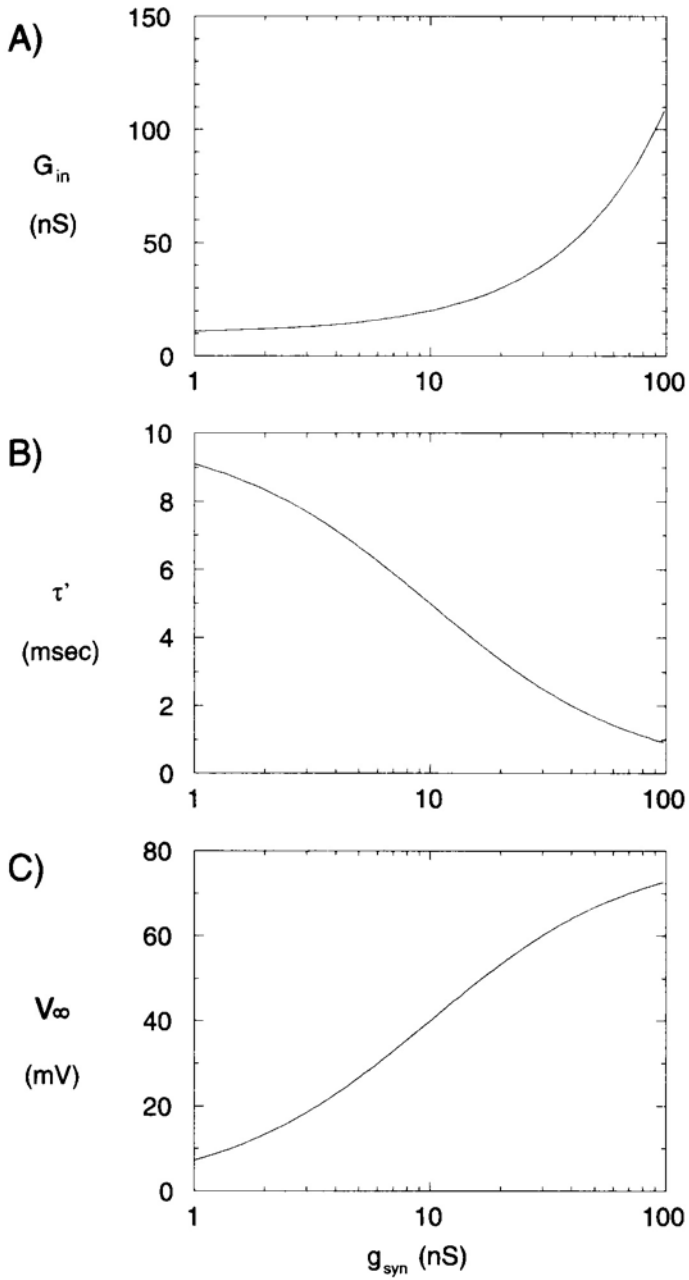

Fig. 1.9 SYNAPTIC INPUT, SATURATION, AND THE TIME CONSTANT The effect of varying the synaptic input conductance on **(A)** the input conductance G_{in} (Eq. 1.24), **(B)** the membrane time constant τ' (Eq. 1.25), and **(C)** the steady-state change in membrane potential V_∞ (Eq. 1.26) in a single-compartment model (Fig. 1.7A) as a function of g_{syn}. Conceptually, if we assume an excitatory synapse (with $E_{syn} = 80$ mV) and a fixed peak amplitude of $g_e = 1$ nS, the x axis is logarithmic in the number of synapses involved in the overall synaptic event. Note that τ' as well as G_{in} will increase irrespective of whether the synapses are depolarizing, shunting, or hyperpolarizing. The fact that the input to neurons comes in the form of a change in the membrane conductance implies that the very structure of the neuronal hardware changes with the input, since the dynamics of the cell speeds up in the presence of strong synaptic input.

(from Koch)

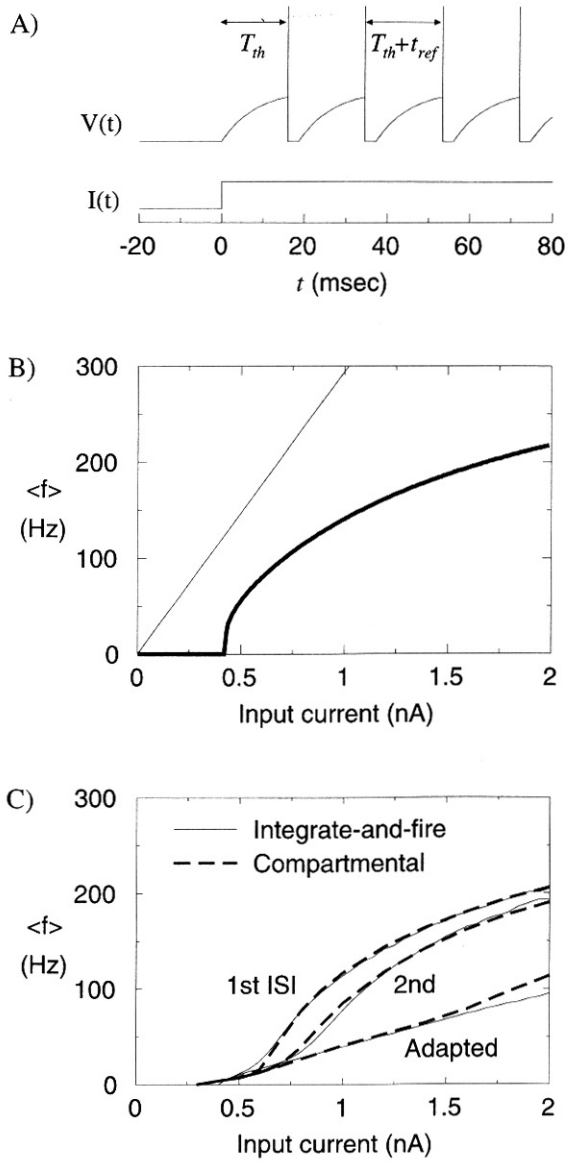

Fig. 14.3 SPIKING IN A LEAKY INTEGRATE-AND-FIRE MODEL Average firing frequency, determined as the inverse of the interspike interval, as a function of the amplitude of a maintained current input, for a leaky integrate-and-fire unit (Fig. 14.2B). **(A)** Exemplar trace of such a unit receiving a current step input with $I = 0.5$ nA. Before the membrane potential has time to reach equilibrium, the unit spikes. $V_{\text{th}} = 16.4$ mV, $C = 0.207$ nF, $R = 38.3$ MΩ, and $t_{\text{ref}} = 2.68$ msec. **(B)** f–I or *discharge* curve for the same leaky unit with refractory period (Eq. 14.11). The slope is infinite at threshold ($I_{\text{th}} = V_{\text{th}}/R$). The firing rate saturates at $1/t_{\text{ref}}$. For comparison, the f–I curve of the nonleaky unit without refractory period with constant slope $1/(V_{\text{th}}C)$ is superimposed. **(C)** An adapting conductance (with $G_{\text{inc}} = 20.4$ nS and $\tau_{\text{adapt}} = 52.3$ msec) is added to the leaky integrate-and-fire unit (see Fig. 14.2C) and the resulting f–I curve is compared against the discharge curve of the biophysical detailed compartmental model of the layer 5 pyramidal cell (Fig. 17.10). The degree of matching between simple and very complex models is quite remarkable and supports our contention that suitably modified integrate-and-fire models do mimic numerous aspects of the behavior of neurons. Adaptation is already evident when considering the first interspike interval (between the first and second spikes). Adaptation linearizes the very steep f–I curve around I_{th} (compare with B).

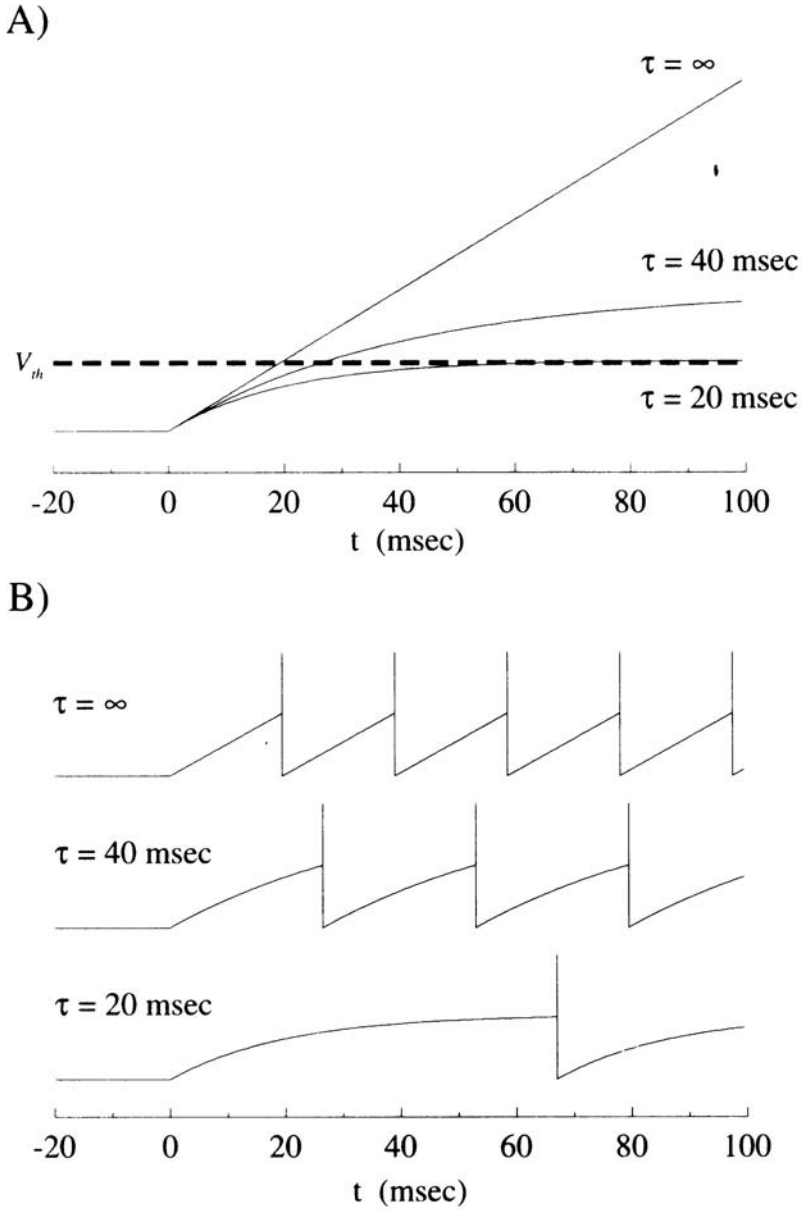

Fig. 14.7 Response Time in Spiking and Firing Rate Models Effect of changing the membrane time constant on **(A)** a nonspiking (or firing rate) neuron and **(B)** an integrate-and-fire neuron. The input current to the cell changes from zero to 0.85 nA at time 0. Subthreshold parameters were the same in both panels ($C = 1$ nF; R was varied from 20 MΩ to infinity; no refractory period). The subthreshold voltage of the integrate-and-fire model in **B** is exactly the same as for the nonspiking model in **A** until the threshold V_{th} (dashed line in **A**) is crossed. Increasing R increases the rate of change of voltage, but also increases the equilibrium voltage. Nonspiking neurons therefore converge more slowly as the time constant increases. As $\tau \rightarrow \infty$ (when the leaky integrate-and-fire unit turns into a perfect one) the integrate-and-fire model responds earlier.

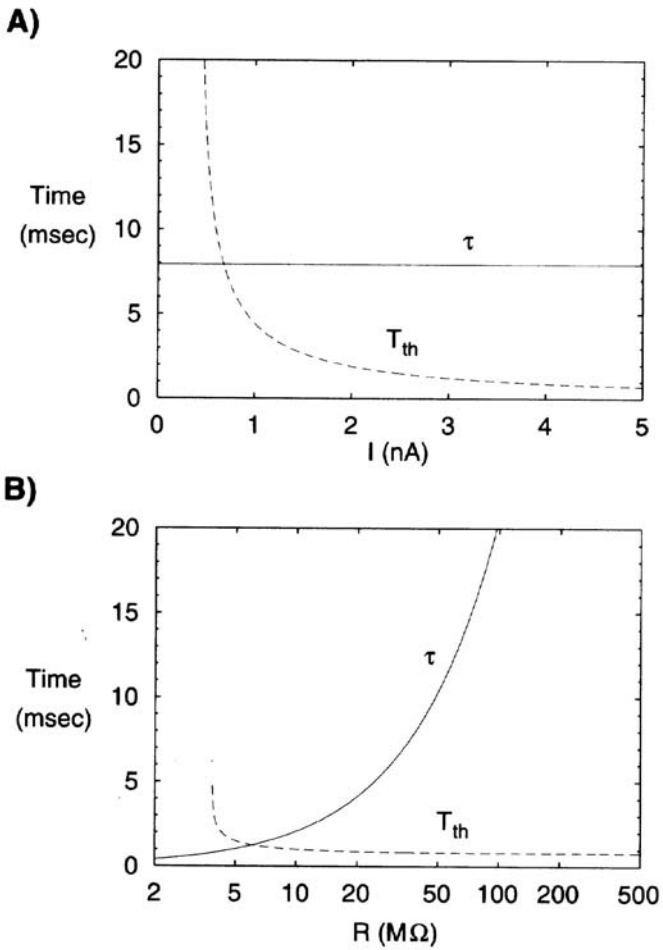

Fig. 14.5 INTEGRATE-AND-FIRE UNITS CAN RESPOND MUCH FASTER THAN τ Membrane time constant $\tau = RC$ of a leaky integrate-and-fire unit and the time T_{th} it takes such a unit, starting at $V = 0$, to reach V_{th} and spike (Eq. 14.10). **(A)** As the amplitude of the injected current increases, the unit can spike very rapidly. The true time to spike is $\leq T_{\text{th}}$, since the unit's initial state is usually $V > 0$. The parameters are as in Fig. 14.3A. **(B)** Input resistance R is varied over two orders of magnitude. As τ diverges, T_{th} converges to CV_{th}/I, the time it takes for the voltage across a capacitance to reach V_{th}. While this may be counterintuitive, it follows from the fact that T_{th} is the time it takes to reach a fixed threshold value, while τ dictates the approach toward a steady-state value beyond V_{th}. The injected current $I = 4.3$ nA. All else as in the upper panel. For small values of R, the current fails to reach I_{th} and T_{th} diverges.